P379 RADIOSYNTHESIS AND RADIOPHARMACOLOGICAL CHARACTERIZATION OF N.C.A. SODIUM (^{18}F)FLUOROACETATE IN TUMOR BEARING MICE

R. BERGMANN, S. RICHTER and F. WÜST

Institut für Radiopharmazie, Forschungszentrum Dresden-Rossendorf, Dresden, Germany

Introduction: [^{18}F]Fluoroacetate is discussed as an alternative to the well-established PET radiotracer [^{11}C]acetate for the diagnosis and treatment monitoring of prostate cancer. The first automated synthesis of [^{18}F]fluoroacetate was reported very recently by Sun and co-workers [1]. Herein we describe an alternative convenient remotely-controlled synthesis of no-carrier-added sodium [^{18}F]fluoroacetate and its radiopharmacological evaluation in tumor bearing mice.

Experimental: Three ethyl esters and three tert.-butyl esters containing either a methanesulfonyloxy- (OMs), p-toluenesulfonyloxy- (OTs) or p-nitrobenzene-sulfonyloxy (ONs) leaving group were investigated as labeling precursors.

Results and Discussion: The optimized radiosynthesis of n.c.a. sodium [^{18}F]fluoroacetate was performed in two steps: (1) Incorporation of fluorine into (methanesulfonyloxy)-acetic acid tert.-butyl ester 1 as the superior labeling precursor in acetonitrile at 100°C for 5 min followed by (2) acidic hydrolysis of the resulting [^{18}F]fluoroacetic acid tert.-butyl ester at 100°C for 10 min to afford [^{18}F]fluoroacetic acid. Several consecutive purification steps using anion exchange cartridges (Alltech Maxi-Clean SAX) and Sep-Pak neutral alumina cartridges gave sodium [^{18}F]fluoroacetate in very reproducible radiochemical yields (20-25%, decay-corrected, n=20) in high radiochemical purity (>95%) within 50 min (Fig. 1).

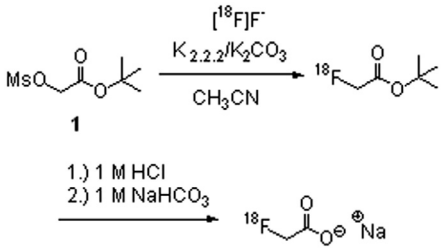

Fig. 1. Radiosynthesis of [^{18}F]fluoroacetate.

Radiopharmacological studies were performed using rats and tumor bearing mice. Metabolism studies in arterial blood showed no metabolites after 60 min p.i. [^{18}F]Fluoroacetate was readily accumulated in HT-29 tumors (tumor/muscle 1.75 ± 0.20 mean ± SEM, n=6) as shown in small animal PET studies (Fig. 2).

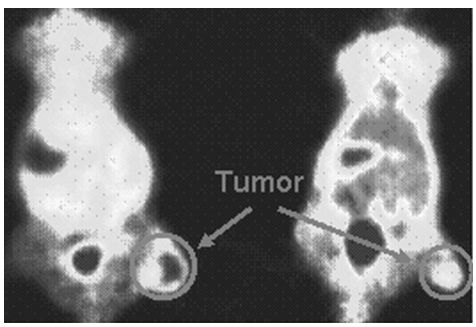

Fig. 2. Small animal PET (45 min p.i.).

Conclusion: The robust and reproducible remotely-controlled two step/one pot synthesis of [^{18}F]fluoroacetate starting from readily available (methanesulfonyloxy)-acetic acid tert.-butyl ester 3a as a novel labelling precursor represents an alternative to the published procedures. A comparing discussion of data obtained with [^{11}C]acetate in rats and mice will be presented.

References: [1] L.-Q. Sun et al. Nucl. Med. Biol., 2006, 33, 153-158.

Keywords: 18F-Labeling, [^{18}F]Fluoroacetate

P380 MICROPET IMAGING WITH (^{18}F)FDDNP AND (^{18}F)FDG IN A TRANSGENIC MOUSE MODEL OF ALZHEIMER'S DISEASE

O. LANGER[1,2], C. KUNTNER[1], T. WANEK[1], M. BAUER[2], M. MANDLER[3], P. ANGELBERGER[1], M. MUELLER[2] and H. KVATERNIK[1]

[1]Dept. of Radiopharmaceuticals, Austrian Research Centers, Seibersdorf, Austria; [2]Dept. of Clinical Pharmacology, Medical University of Vienna, Austria; [3]AFFiRiS GmbH, Vienna, Austria

Introduction: Mouse models transgenic for the human amyloid precursor protein are commonly used in the development of new therapeutics against Alzheimer's disease (AD). MicroPET imaging potentially allows for performing longitudinal studies to assess *in vivo* the efficacy of new AD therapeutics. We evaluated the usefulness of microPET with the beta-amyloid (Aβ) probe [^{18}F]FDDNP[1] and with [^{18}F]FDG for detection and quantification of pathological changes that occur in the brains of Tg2576 mice.

Experimental: [^{18}F]FDDNP and [^{18}F]FDG microPET scans were performed with a Siemens microPET Focus 220 scanner in Tg2576 mice (n=6) and age-matched wild-type litter mates (n=5, age:13-15 months). Retention of [^{18}F]FDDNP in Aβ-rich target brain regions (frontal and parietal cortex, hippocampus) was quantified in terms of the distribution volume (*DV*) with cerebellum as reference region calculated by Logan graphical analysis. For [^{18}F]FDG, target-region-to-cerebellum ratios were calculated from a 30-min static image recorded at 1 h after tracer injection.

Results and Discussion: For [^{18}F]FDDNP, peak brain uptake of radioactivity was in all examined brain regions significantly lower in transgenic as compared to wild-type mice (-25% to -41%, P<0.05, Student's t-test). Moreover, late (>35 min) target-region-to-cerebellum ratios as well as [^{18}F]FDDNP *DV*s were decreased by 7-10% in Tg2576 *versus* wild-type mice with significant differences found in parietal cortex. Also for [^{18}F]FDG, target-region-to-cerebellum ratios were lower in all examined brain regions of Tg2576 mice (parietal cortex: -6.1%, hippocampus: -10.0%, frontal cortex: -22.3%). None of the differences in [^{18}F]FDG retention was statistically significant, which was in all likelihood related to the rather high variability of the data (coefficient of variation: 9-23%).

Conclusion: Our data suggest that [^{18}F]FDDNP is not suited for the quantification of Aβ in Tg2576 mice. The lower brain uptake of [^{18}F]FDDNP in transgenic mice might be explained by decreased cerebral perfusion due to β-amyloidosis. Our findings are in line with previous data showing that another Aβ probe ([^{11}C]PIB) is also not suitable for Aβ quantification in transgenic mice, which has been attributed to lower Aβ binding site densities in the transgenic mouse as compared to the AD brain.[2,3] Reduction of [^{18}F]FDG brain retention in transgenic mice points to regionally decreased glucose metabolism and deserves further investigation in larger sample sizes.

References: [1] Shoghi-Jadid K *et al* Am J Geriatr Psychiatry 10:24 (2003). [2] Klunk WE *et al* J Neurosci 25:10598 (2005). [3] Ye L *et al* Biochem Biophys Res Commun 347:669 (2006).

Keywords: [^{18}F]FDDNP, [^{18}F]FDG, MicroPET, Alzheimer, Tg2576 Mice

P381 COMPARISON OF BIO-DISTRUBUTION OF ORAL AND INTRAVENOUS ADMINISTERED 2-(^{18}F)-FLUORO-DEOXY-GLUCOSE (^{18}F-FDG) IN WISTAR RATS. CAN ^{18}F-FDG BE ADMINISTERED ORALLY IN CERTAIN CLINICAL CIRCUMSTANCES?

M.G.R. RAJAN, P.R. CHAUDHARI, N. LAKSHMINARAYAN and P.S. SONI

Laboratory Nuclear Medicine Section, Bhabha Atomic Research Centre, Mumbai, Maharashtra, India

Introduction: 2-[^{18}F]Fluoro-deoxy-glucose (^{18}F-FDG), a glucose analogue, is largely used as a PET tracer in neurology, cardiology and oncology, and in the latter, to assess the response to therapy. Because of the short half of the ^{18}F, it is necessary to complete its synthesis and quality control procedures, including sterility and endotoxin tests, in the shortest possible time. In this study, we have compared the bio-distribution of ^{18}F-FDG administered by oral and intravenous route in Wistar rats. Oral radiopharmaceuticals do not require the costly and difficult endotoxin detection in the product.

Experimental: The study was designed to compare the bio-distribution of ^{18}F-FDG administered by oral and intravenous route in Wistar rats fasted overnight. The rats (n=18) were divided in two groups. One group was administered ^{18}F-FDG orally and the other intravenously. From each group, three animals were sacrificed at 30min, 1h and 3h post-injection respectively. Thereafter, the organs were dissected and counted for the presence of the tracer and percentage uptake with reference to total injected activity was calculated.

Results and Discussion: The percentage uptake in the oral and intravenous administration group at 30min, 1hr and 3hr post injection as shown in Table 1.

Table 1. Comparison of biodistribution of oral and intravenous administered ^{18}F-FDG

Organs	30min post-injection		1h post-injection		3h post-injection	
	Oral	IV	Oral	IV	Oral	IV
Blood	3.32	7.65	4.07	3.91	1.75	1.11
Bone	1.27	6.1	2.19	8.3	6.29	8.49
Muscle	6.08	2.78	11.45	17.23	13.49	15.33
Brain	0.67	2.68	1.49	3.65	2.77	2.36
Heart	0.13	0.3	0.26	0.45	0.35	0.36
Liver	0.07	3.44	0.25	2.07	0.45	1.20
Stomach	39.32	0.72	21.35	0.90	0.87	0.68
Small Intestine	26.20	5.95	28.21	7.89	8.53	5.84
Kidney	0.70	1.46	0.70	1.04	0.67	0.63

Conclusion: Our finding suggests that at 3h post-injection, the biodistribution of ^{18}F-FDG in both the groups is comparable and, therefore, the oral route appears to be as effective as the intravenous route. Waiting for 3h prior to scanning may be beneficial as the signal to noise ratio improves. This may be of value particularly in geriatric subjects. It will also eliminate the cost and time taken for estimation of bacterial endotoxin in the final product. Further, oral administration can be done soon after synthesis saving decay losses. 'Parametric release' criteria, essential for PET-radiopharmaceuticals, would be simpler. Besides, it can provide ease to patients and reduction in occupational radiation exposure to personnel administering the radioactivity.

Keywords: [^{18}F]Fluorodeoxyglucose, Animal Biodistribution

P382 MICROPET AND HISTOLOGY STUDIES OF THE USE OF A GEMCITABINE BISPHOSPHONATE CONJUGATE (GEM/BP) AS TARGETED BONE-SPECIFIC THERAPEUTIC AGENT IN A HUMAN BREAST CANCER BONE METASTASES MODEL

A.A. EL-MABHOUH [1], P.N. NATION [2], E. POSTEMA [2], T. RIAUKA [2], S. MCEWAN [2] and J.R. MERCER [1,2]

[1]Faculty of Pharmacy and Pharmaceutical Sciences, University of Alberta, Edmonton, AB, Canada; [2]Faculty of Medicine, University of Alberta, Edmonton, AB, Canada

Introduction: The gemcitabine bisphosphonate conjugate (Gem/BP) was synthesized to target the bone and to provide bone-specific chemotherapy in metastatic disease. A previous study with ^{99m}Tc-Gem/BP proved that this conjugate has a high affinity to bind to bone when injected in healthy Balb/C mice.

Experimental: We examined the effects of Gem/BP in a bone metastasis model in nude mice (Balb/C-nu/nu) in which intracardiac injection of the human breast cancer cell line MDA-MB-231Bo (MDA-231Bo) produced osteolytic bone metastasis. Starting at one day after the inoculation of MDA-231Bo cells into the left heart ventricle, 4 doses of Gem/BP (27 mg/kg) or Gemzar® (gemcitabine) (15 mg/kg) were administered intravenously at 3 day intervals. Another group of mice received no treatment and was used as a control group. High resolution X-rays radiographs were collected on day 26 and before the end of the experiment on day 33. ^{18}F-fluoride microPET whole mouse images were collected on day 30.

Results and Discussion: MicroPET images showed that Gem/BP reduced the number and the size of bone metastasis lesions relative to the control group. The histological examinations of the proximal humerus of the untreated and Gemzar® control groups revealed that most of the cancellous bone had been replaced by the metastatic cancer lesions, the bones medullary cavity contained large metastatic mass, the trabeculae bones have been completely eroded and replaced by malignant cells and the bone marrows were aggressively invaded by the cancer cells. On the contrary, Gem/BP treated mice showed few small wedge-shaped metastases under the periosteum of the outer cortex. Significantly, neither the medullary cavity nor the bone marrows are invaded by the cancer cells.

Conclusion: These data suggest that Gem/BP should be considered as a potential drug to be used in the treatment of bone metastases.

Acknowledgement: The authers are grateful for the Canadian Breast Cancer Foundation for their financial support.

Keywords: MicroPET, Gemcitabine, Bisphosphonate, Bone Metastases, MDA-MB-231Bo

P383 GENERIC MODELS FOR ASSESSING RADIATION DOSES FROM RADIOPHARMACEUTICALS LABELLED WITH ^{11}C OR ^{18}F: ARE THEY ACCEPTABLE?

D.M. TAYLOR

School of Chemistry, Cardiff University, Cardiff, Wales, United Kingdom

Introduction: For many of the [^{11}C]- and [^{18}F]-radiopharmaceuticals now being developed for positron emission tomographic (PET) receptor studies in human organs the available biokinetic data are insufficient for calculation of the realistic radiation dose estimates necessary for clinical application. Thus, default models for [^{11}C]- and [^{18}F]-labelled substances that would predict the internal dose with sufficient accuracy for general radiation protection purposes would be useful. Generic models for [^{11}C]- and [^{18}F]-labelled amino acids and for [^{11}C]-brain receptor substances have been proposed (1; 2). A similar generic model for [^{18}F]-receptor agents based on consideration of the compound-specific dosimetry of 18 [^{18}F]-receptor agents, is discussed here.

Experimental: This [^{18}F]-model assumes that, of the injected activity 8% deposits in liver, 2% in brain, lungs and red bone marrow and 1% in the kidneys and is lost with a biological half-time of 12 hours. Urinary excretion is assumed to be 30%. Radiation doses for this model, calculated for a reference adult using the OLINDA dose code.

Results and Discussion: The effective dose calculated for this model is 16 m Sv/MBq. The corresponding mean effective dose for the 18 compound-specific doses was 17$\pm$1 mSv/MBq.

Comparison of the absorbed doses to individual tissues calculated using the generic, amino acid or receptor models, referenced or described here, suggests that the predicted doses are generally within a factor of 2-3 of those predicted by the [^{11}C-] or [^{18}F]-compound-specific models from which they were derived. This margin of uncertainty is considered to be acceptable for general, prospective radiological protection purposes.

Conclusion: The use of such generic models would avoid the necessity for carrying out studies in experimental animals just to provide biokinetic data for compounds which, after a few trials, may prove to be of little clinical interest.

However, these default models are not suitable for retrospective dosimetry. When it is necessary to assess the dose actually received by a particular patient every attempt should be made to obtain patient-specific, radiopharmaceutical-specific biokinetic information.

References: [1] Taylor, D.M. (2000) Generic models for radionuclide dosimetry: ^{11}C-, ^{18}F- or ^{75}Se-labelled amino acids. *Appl. Radiat. Isot.* **52**, 911-922. [2] Nosslin, B. Johansson, L., Leide-Svegborn, S., Liniecki, J., Mattsson, S and Taylor, D.M. (2003) A generic model for [^{11}C]-labelled radiopharmaceuticals for imaging receptors in the human brain. *Rad. Prot. Dosim.* **105**(1-4), 587-591.

Acknowledgement: The author wishes to thank his colleagues on the ICRP TaskGroup on Doses to Patients from Radiopharmaceuticals for helpful discussions.

Keywords: Radiopharmaceutical Dosimetry, Generic Models, Carbon-11; Fluorine-18

P384 INTRAVENOUS AMPHETAMINE ADMINISTRATION DOES NOT AFFECT METABOLISM OF (^{11}C)RACLOPRIDE

R.C. SCHUIT, G. LUURTSEMA, H.N.J.M. GREUTER, N.H. HENDRIKSE, A.D. WINDHORST, B.N.M. VAN BERCKEL and A.A. LAMMERTSMA

Department of Nuclear Medicine & PET Research, VU University Medical Centre, Amsterdam, Netherlands

Introduction: The effects of amphetamine administration on metabolism of [C-11]raclopride were evaluated in five healthy volunteers who participated in a baseline scan and a post-amphetamine (0.3 mg/kg) scan on the same day.

Experimental: [C-11]raclopride was administrated using a bolus plus continuous infusion paradigm. During the second scan, amphetamine was administered two minutes prior to [C-11]raclopride infusion. During both scans, 5 discrete blood samples were withdrawn between 40 and 80 minutes after administration of [C-11]raclopride. First, plasma to blood ratios were determined. Next, at 3 time points, metabolite analysis was performed in the following manner. 1 ml of plasma was acidified with 6M HCl (20μl/ml), diluted with 2 ml of water, and passed over an OASIS HLB (60 mg) SPE cartridge. Next, the SPE cartridge was washed with 3 ml of water. Finally, [C-11]raclopride and its non-polar metabolites were eluted with 1.5 ml of methanol and 1.5 ml of 0.4% DIPA in water. The combined organic fractions were vortexed and injected onto the HPLC system (Phenomenex Gemini column, C18, 5 μm, 250*10 mm). Gradient: methanol (A) and 0.4% DIPA in water (B) (%B: 0-4 min, 80%; 4-12 min, 80-20%; 12-20 min, 20%; 20-21 min, 20-80%; 21-25 min, 80%) at 2.0 mL/min. 30 s fractions were collected and counted for radioactivity using a Wallac 1470 Wizard®. Data were transferred into MS Excel and an HPLC chromatogram was reconstructed.

Results and Discussion: The retention time of parent [^{11}C]raclopride was 15.3 minutes, whilst the only metabolite formed had a retention time of 12.8 min. No polar fraction was found, indicating that demethylation did not occur. The total recovery of the SPE and HPLC analysis system was >95%. Results of activity concentration and metabolite fraction measurements are shown in table 1.

Table 1. Concentrations of [^{11}]raclopride in whole blood (WB) and plasma (Pl) before and after administration of amphetamine (N = 5), together with parent fractions in plasma

Time (min)	Baseline			After administration of amphetamine		
	Conc. WB (kBq/mL)	Conc. Pl (kBq/mL)	% Parent	Conc. WB (kBq/mL)	Conc. Pl (kBq/mL)	% Parent
40	2.79±0.68	4.57±1.16	80.9±7.2	2.75±0.36	4.51±0.67	78.0±8.9
50	2.77±0.68	4.54±1.15		2.72±0.34	4.47±0.61	
60	2.77±0.70	4.49±1.14	78.5±6.8	2.77±0.37	4.52±0.63	76.4±10.4
70	2.86±0.72	4.66±1.20		2.81±0.40	4.62±0.62	
80	2.91±0.74	4.72±1.23	77.1±11.0	2.85±0.39	4.68±0.66	78.2±10.3

Conclusion: Amphetamine administration did not affect the metabolic profile of [^{11}C]raclopride.

Keywords: Amphetamine, Raclopride, Positron Emission Tomography, Metabolites

P385 PLASMA METABOLITES OF ([11]C)R107474 IN RHESUS MONKEYS

R.C. SCHUIT, J.S. SCHEPERS, M.P.J. MOOIJER, G. LUURTSEMA, P.J. KLEIN, R.W. KLOET, J.E. LEYSEN, A.A. LAMMERTSMA and A.D. WINDHORST

Department of Nuclear Medicine & PET Research, VU University Medical Centre, Amsterdam, Netherlands

Introduction: [[11]C]R107474 is a potent and relatively selective α2-adrenoceptor antagonist [1], which is under investigation as a ligand for positron emission tomography (PET). This investigation involves studies in Rhesus monkeys. For proper quantification and kinetic modelling of acquired PET data, a metabolite corrected plasma input function is required. It is known that, in rats and humans, [[11]C]R107474 metabolises into two compounds, R125460 and R129144 (figure 1). Therefore, a method was developed for measuring these metabolites of [[11]C]R107474 in arterial blood samples.

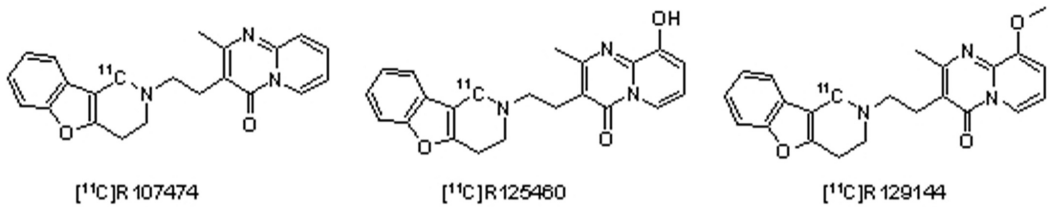

Fig. 1 [[11]C]R107474 and its metabolites.

Experimental: From each arterial blood sample, a maximum of 300 mg of plasma was acidified with 3 μl of 6 M HCl per 300 mg of plasma and, after dilution with 2 ml of water the solution was loaded onto a Sep-Pak tC18 SPE cartridge. After washing with 4 ml of 0,9% NaCl, the analytes were eluted with 2 ml of methanol. 1 ml of the eluate was injected onto an HPLC system (Phenomenex Gemini C18, 5 μm, 250*10 mm) with MeCN/H2O/DIPA (55/45/0.2) as mobile phase at a flow rate of 2.5 ml/min. The other 1 ml was used to calculate total recovery. Using this HPLC system all three compounds were baseline separated. Retention times were 15.3, 13.7 and 4.2 minutes for R107474, R129144 and R125460, respectively.

Results and Discussion: Total recovery of the SPE/HPLC was always >90%. In figure 2 results of the [C-11]R107474 plasma metabolite measurements are presented. One hour after injection 26 ± 7% of plasma radioactivity was due to parent [[11]C]R107474. The main metabolite was [[11]C]R125460, representing 58 ± 9% of total radioactivity. Metabolite [[11]C]R129144 was not detected in plasma.

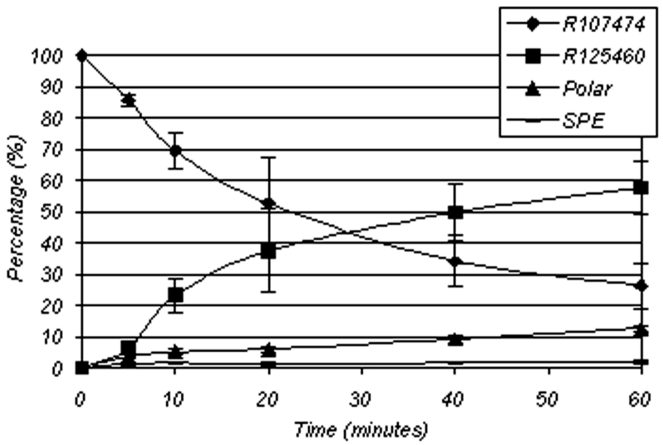

Fig. 2. Fractions of [[11]C]R107474 and its radioactive metabolites in arterial plasma of Rhesus monkey as function of time.

Conclusion: Radiolabelled metabolites of [[11]C]R107474 were observed in Rhesus monkey plasma. The main metabolite found was [[11]C]R125460.

References: [1] Van der Meij et al., Bioorg Med Chem, 2006, 14: 4526-4543.

Keywords: Alpha-2 Receptor, R107474, Positron Emission Tomography, Metabolites

P386 α_{2C}-ADRENOCEPTOR AUTORADIOGRAPHY IN HUMAN BRAIN

V. FAGERHOLM [1], J. ROKKA [1], L. NYMAN [2], J. SALLINEN [2], M. HAAPARANTA [1] and J. HIETALA [3]

[1]Turku PET Centre, University of Turku, Turku, Finland; [2]Orion Corporation, Turku, Finland; [3]Department of Psychiatry, University of Turku, Turku, Finland

Introduction: Three α_2-adrenoceptor subtypes, α_{2A}, α_{2B}, and α_{2C}, mediate many of the physiological effects of noradrenaline and adrenaline. The α_{2C}-adrenoceptor is implicated in several neuropsychiatric disorders including ADHD, depression, and schizophrenia. In rodent brain, the highest densities of α_{2C}-adrenoceptors are found in the striatum and the olfactory tubercles. In human brain, the distribution of the α_{2C}-adrenoceptor is still largely unknown, due to the poor subtype-selectivity of the available α_2-adrenoceptor ligands. The purpose of this study was to assess the presence of α_{2C}-adrenoceptors in human brain in order to provide a basis for target validation of putative new α_{2C}-adrenoceptor-selective PET radioligands.

Experimental: Competition binding receptor autoradiography was performed on rat and human post-mortem brain sections using the subtype-non-selective α_2-adrenoceptor antagonist [Ethyl-^{3}H]RS79948-197 and the recently characterized α_{2C}-adrenoceptor-selective antagonist JP-1302 (Orion Pharma, Turku, Finland). The brain sections were incubated for 1.5 hours with the radioligand and various concentrations of JP-1302, and were thereafter washed for 1 hour in cold buffer solution and rinsed in cold water. Digital autoradiography was performed and competition binding curves were generated for striatum, cerebral cortex, and cerebellum. Pharmacological receptor binding parameters were obtained by non-linear least square regression analysis.

Results and Discussion: In rat and human striatum, both high- and low-affinity binding sites were present. In cortex and cerebellum, only a low-affinity binding site was detected in both species. The apparent JP-1302 K_i values of the high- and low-affinity binding sites were in good agreement with the JP-1302 K_i values previously determined from recombinant cell-lines expressing α_{2C}- and α_{2A}-adrenoceptors, respectively. The results suggest the presence of a significant portion of α_{2C}-adrenoceptors in addition to α_{2A}-adrenoceptors in striatum, while the α_{2A}-adrenoceptor predominates in cerebral cortex and cerebellum. Since the α_{2C}-adrenoceptor subtype distribution pattern thus appears to be conserved between rodents and humans, the results obtained from studies on the role of the α_{2C}-adrenoceptor in rodent models of psychiatric disorders are likely to be relevant for human diseases as well.

Conclusion: The striatal location of α_{2C}-adrenoceptors in human brain provides a rationale for the development of α_{2C}-adrenoceptor-selective PET radioligands, with the notion that such ligands may advance the understanding of neuropsychiatric disorders involving the brain noradrenergic system.

Keywords: Adrenergic Receptors, [Ethyl-3H]RS79948-197, JP-1302, Striatum, Receptor Autoradiography

P387 PLASMA METABOLITES OF (^{11}C)PIB AND (^{18}F)FDDNP

K. TAKKENKAMP, G. LUURTSEMA, H.N. GREUTER, R.C. SCHUIT, A.D. WINDHORST, N.H. HENDRIKSE, N. TOLBOOM, B.N. VAN BERCKEL and A.A. LAMMERTSMA

Department of Nuclear Medicine & PET Research, VU University Medical Centre, Amsterdam, Netherlands

Introduction: [^{11}C]PIB and [^{18}F]FDDNP are PET tracers for imaging amyloid plaques in Alzheimer's Disease. To quantify specific binding of these tracers, a metabolite corrected plasma input function is required. The purpose of the present study was to develop fast, reliable and sensitive plasma metabolite analysis methods for both tracers.

Experimental: For measuring [^{11}C]PIB and its radioactive metabolites in plasma, an on-line solid phase extraction (SPE), combined with HPLC, analysis method was developed. A tC_{18} SPE column was used in combination with a 5μm Gemini HPLC column (250 x 4.6 mm). A 1 ml HPLC loop was filled with plasma and loaded onto a SPE column using 0.01 M $(NH_4)_2HPO_4$. [^{11}C]PIB and its radioactive metabolites were trapped on the SPE column**.** Subsequently, this SPE column was eluted directly onto the HPLC column with a mobile phase of acetonitrile/10 mM NH_4OAc (50/50 v/v) and a flow of 2.5 ml·min^{-1}. For measuring [^{18}F]FDDNP and its radioactive metabolites, 1 ml of water was added to 2 ml of plasma. First, the diluted plasma was loaded onto an activated Sep-Pak® (1 g) plus tC_2 cartridge using a vacuum manifold. After rinsing the cartridge with 3 ml of H_2O, [^{18}F]FDDNP and its radioactive metabolites were eluted from the cartridge with 1.5 ml MeOH and 0.5 ml water containing 0.2% of diisopropylamine. The eluted fraction was weighed and 1 ml was injected onto an HPLC system (Phenomenex Gemini 5μm C18 110Å) with MeOH/H_2O/DIPA (75/25/0.2%v/v) as eluent at a flow of 3 ml·min^{-1}.

Results and Discussion: Using both SPE/HPLC systems, total recovery of [^{11}C]PIB and [^{18}F]FDDNP from plasma was always > 90%. For both SPE/HPLC systems, parent compound and metabolites were baseline separated. Both [^{11}C]PIB and [^{18}F]FDDNP underwent extensive metabolism, as shown in Table 1 (* < limit of quantification). In combination with the biological clearance of these tracers, this leads to large statistical uncertainties in the measurements of the latest samples.

Table 1. Mean (± SD) parent fraction in plasma (n=7).

Time (min)	% [^{11}C]PIB	SD	% [^{18}F]FDDNP	SD
0	100.0	0.0	100.0	0.0
5	49.5	22.8	24.9	13.7
10	27.2	13.6	10.5	6.5
20	13.3	7.3	5.2	3.4
40	6.5	3.8	3.1	2.3
60	4.3	2.4	1.4	0.9
75	3.3*	2.2	1.1	0.9
90	2.9*	2.1	1.2	1.0

Conclusion: Two different methods were developed for measuring fractions of [^{11}C]PIB, [^{18}F]FDDNP and their radioactive metabolites in plasma. Both methods used SPE for sample preparation in combination with HPLC analysis. Due to rapid metabolism, measurements beyond 60 minutes suffer from large statistical uncertainties, especially in case of [^{11}C]PIB.

Keywords: [^{11}C]PIB, [^{18}F]FDDNP, Plasma, Metabolite Analysis, PET

P388 ALTERNATIVE APPROACH FOR MEASURING NON CARRIER ADDED *(R)*-([11]C)VERAPAMIL IN PLASMA

G. LUURTSEMA [1], R. HONEYWELL [2], R.C. SCHUIT [1], G.J. PETERS [2] and A.A. LAMMERTSMA [1]

[1]Department of Nuclear Medicine and PET Research, VU University Medical Centre, Amsterdam, Netherlands; [2]Department of Medicinal Oncology, VU University Medical Centre, Amsterdam, Netherlands

Introduction: *(R)*-[[11]C]verapamil is an accepted tracer of functional P-gp in the BBB. For quantification, a metabolite corrected plasma input function is required. Usually, the fraction of parent compound is determined using radioactivity measurements of samples from SPE combined with HPLC. Although this method is sensitive, it is restricted by the half-life of ^{11}C, requiring immediate processing of samples. An alternative approach that would circumvent these problems is to measure the concentrations of stable parent compound directly.

Experimental: Plasma samples from five patients taken 5 and 40 minutes after injection of 370 MBq *(R)*-[[11]C]verapamil were used. For LC-MS/MS analysis, samples were prepared by adding [methyl-d_3] verapamil (0.022 nmol) to 3 ml plasma. Each sample was diluted with 2.5 ml of 0.1 M phosphate buffer (pH 7.4). The plasma–buffer mixture was loaded onto an SPE cartridge. After washing with 2 ml of water, the SPE was eluted with methanol/triethylamine/isoamyl alcohol (98.75/0.25/1.00). The eluant was evaporated and dissolved in 60 μl of mobile phase. 1μl of the sample was injected onto an API 3000. The detection of verapamil was performed in positive TIS mode using the transition pairs of 458/165 (d_3-verapamil) and 455/165 (verapamil). The LC separation was performed at a flow rate of 0.1 ml/min on a 100x10, 3.5 μm C18 XTerra column. Finally, the same plasma samples were also analysed using RA-HPLC. Using the specific activity of labelled verapamil, concentrations were calculated and compared with LC-MS/MS data.

Results and Discussion: Data from both techniques are presented in table 1.

Table 1. Plasma verapamil concentration after tracer dose injection

Plasma sample		Concentration (pMol/ml)	
Patient no.	Time p.i. (min)	LC-MS/MS	RA-HPLC
1	5	0.083±0.013	0.053
1	40	0.048±0.011	0.018
2	5	0.119±0.021	0.061
2	40	0.055±0.001	0.028
3	5	0.230±0.019	0.109
3	40	0.061±0.010	0.030
4	5	0.193±0.002	0.130
4	40	0.094±0.001	0.047
5	5	0.181±0.007	0.060
5	40	0.073±0.004	0.017

Conclusion: The sensitivity of LC-MS/MS is sufficient to allow for measurements of plasma parent verapamil concentrations following a tracer dose injection of *(R)*-[[11]C]verapamil. This method should be investigated further by assessing its ultimate effect on deriving the volume of distribution of verapamil from dynamic *(R)*-[[11]C]verapamil studies.

Keywords: [[11]C]Verapamil, Plasma, Metabolite Analysis, PET

P389 SCHEDULING OF THE RADIOIODINATED DICHLOROPLATINUM(II)-HISTAMINE COMPLEX IN MAMMARY ADENOCARCINOMA TUMOUR-BEARING MICE

P. GARNUSZEK, M. MAURIN and U. KARCZMARCZYK

Department of Radiopharmaceutuicals, National Medicines Institute, Warsaw, Poland

Introduction: Our previous studies showed that the new radioactive platinum-[*I]histamine complexes posses anticancer activity, inhibiting the tumour growth and extending the survival of mice bearing transplantable colon cancer. In the present work, the treatment scheduling of dichloroplatinum-histamine labelled with I-125 or I-131 were investigated in mammary adenocarcinoma tumour-bearing mice.

Experimental: C3H/W mice with subcutaneous implantation of mammary adenocarcinoma were used for the experiments. The animals were treated with the following preparations: $PtCl_2$Hist (PtHist), $PtCl_2[^{125}I]$Hist (Act.I-125), $PtCl_2[^{131}I]$Hist (Act.I-131), $PtCl_2$His/$PtCl_2[^{125}I]$Hist (PtHist/Act.I-125) and $PtCl_2$His/$PtCl_2[^{131}I]$Hist (PtHist/Act.I-131). The solution of 15% DMF was applied for the control groups. Three treatment protocols were evaluated: *TM1* – long-term, low dose treatment (10 *p.i.* up to 30 day, sum of injected dose: Pt 135 μmol/kg, I-125 210 MBq/kg, I-131 250 MBq/kg); *TM2* – short-term, high dose treatment (4 *p.i.* up to 13 day; Pt 125 μmol/kg, I-125 200 MBq/kg, I-131 200 MBq/kg); *TM3* – long-term treatment with high doses (9 *p.i.* up to 33 day; Pt 255 μmol/kg, I-125 350 MBq/kg and I-131 430 MBq/kg). Antitumour activity was evaluated by calculation of the growth delay factor (GDF), and by comparison of the median survival times.

Results and Discussion: *TM1* protocol: All of the three studied preparations: PtHist, PtHist/Act.I-125 and PtHist/Act.I-131, revealed inhibiting activity on tumour growth and size in comparison to the control group treated with solution of 15% DMF. The most intensive and significant anti-cancer activity was observed for the radioactive complexes, and especially for PtHist/Act.I-125. The GDF of 0.65 was the highest for this group.

TM2: Statistically significant ($P < 0.05$) prolongations of the median survivals were found following treatment with PtHist and PtHist/Act.I-125. Slightly less potent activity was observed for PtHist/Act.I-131, and absolutely no survival improvement were found for the group treated with Act.I-125 and Act.I-131 preparations. Generally, no any statistically significant influence of the applied preparations on tumour growth was observed in the all treated groups.

TM3: An intensive long-term treatment with combined scheduling of PtHist/Act.I-125 and PtHist/Act.I-131 resulted in observation of the highest anticancer effects. The GDF of 1.43, and a significant (*P=0.005*) prolongation of the survival time (Ratio $MS_{tr}/MS_{con}=1.89$) were gained.

Conclusion: The intensive and long-term scheduling of radioactive platinum-histamine resulted in significant inhibition of tumour growth and prolongation of the survival of mice bearing transplanted mammary adenocarcinoma. However, the tumour remission has not been achieved.

Keywords: Dichloroplatinum(II)-[*I]Histamine, Radiochemotherapy, Anticancer Activity, Mammary Adenocarcinoma, Treatment Scheduling

P390 SMALL ANIMAL SPECT/CT FOR IN VIVO EVALUATION OF RADIOTRACERS

F. FORRER [1], C. MUELLER [1], N.U. SCHRAMM [2], C. LACKAS [2], E.P. KRENNING [1] and M. DE JONG [1]

[1]Department of Nuclear Medicine, Erasmus MC, Rotterdam, Netherlands; [2]Central Institute for Electronics, Research Centre Juelich, Juelich, Germany

Introduction: Small animal SPECT has been shown to have high potential in e.g. the development of new drugs or in monitoring of new treatment modalities. In vivo quantification of radiotracers allows following physiological processes over time in the same animal and quantitative comparison of different tracers. The development of multi-pinhole SPECT with higher sensitivity resulted in shorter scanning times, allowing dynamic acquisitions. We investigated the capabilities of a new multi-pinhole SPECT/CT system.

Experimental: The camera (NanoSPECT/CT, Bioscan Inc., Washington D.C.) consists of four detectors, each outfitted with an interchangeable 9-pinhole aperture. The scanning mode is helical for both modalities. Mice and rats were scanned with a variety of tracers emitting photons with different energies ranging from 24 keV(I-125) to 245keV (In-111). Rats with different levels of renal damage were scanned with Tc-99m-DMSA. The kidneys were removed and measured in a gamma counter. After injection of Tc-99m-MAG3 a dynamic SPECT/CT was acquired with a scanning time of 50 s per frame. Pharmacokinetics of radiolabeled somatostatin analogs were followed in a tumor during the first hour, acquiring 30 frames. 24 h p.i. a high resolution SPECT was acquired and correlated with ex vivo autoradiography.

Results and Discussion: The helical scanning mode allows a user-selectable axial field of view of 16 to 290 mm. High quality SPECT/CT images were acquired with all radionuclides. The resolution for SPECT was in the submilimetre range. Good correlation between SPECT and autoradiography was found (Fig. 1). Images could be quantified absolutely to determine uptake in tumor and kidney, respectively. A strong linear correlation between the determined activity in vivo using SPECT and ex vivo using a gamma counter was found. Dynamic scans with Tc-99m-MAG3 allowed reconstruction of a renogram. Due to the good time resolution precise dosimetric calculations on tumors were achievable. I-125-scans in mice allowed separation of the two thyroid lobes.

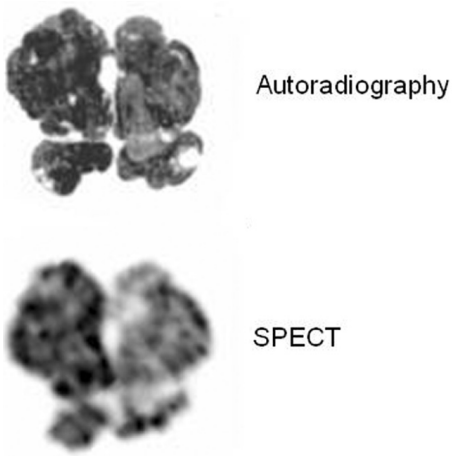

Fig. 1

Conclusion: The NanoSPECT/CT is a highly accurate tool to follow physiological processes in the same animal over time with different tracers. It allows a precise determination of absorbed radioactivity in vivo. This was found in numerous small-animal scans with an array of tracers. Small-animal-SPECT will strongly influence preclinical and clinical research in the near future.

Keywords: SPECT/CT, Small Animal, Pharmacokinetics

P391 BIOLOGICAL EVALUATION OF 6-(^{18}F)FDOPA IN EXPERIMENTAL RATS MODEL OF TUMOR AND INFLAMMATION

O. FEDOROVA, O. KUZNETSOVA and R. KRASIKOVA

Institute of Human Brain RAS, St. Petersburg, Russian Federation

Introduction: Several studies have demonstrated that ^{18}F-radiolabelled amino acids could be suitable radiotracers to distinguish tumor from inflammatory tissues with PET. During last decade the synthetic amino acid tracer *O*-(2'-^{18}F-fluoroethyl)-L-tyrosine ([^{18}F]FET) has been extensively evaluated in animals models. The usefulness of this tracer in differentiating tumor from inflammation was confirmed also in human studies. Recently 6-^{18}F-fluoro-L-DOPA (6-FDOPA), a well established PET agent for evaluation of integrity of dopaminergic system, has shown a great potential for accurate diagnosis of cerebral gliomas [Becherer et al., Eur J Nucl Med Molec Imag 2003; Chen et al., J Nucl Med 2006]. However, to the best of our knowledge, no information is available on the uptake of 6-FDOPA in inflammatory cells. The aim of this study was to investigate the biodistribution of 6-FDOPA comparing with well characterized tumor seeking agent, FDG, in experimental tumor and inflammation tissues in rats model.

Experimental: 6-FDOPA was synthesized by earlier reported method via (*S*)-NOBIN PTC alkylation of achiral Ni^{II} complex with 6-[^{18}F]fluoropiperonyl bromide (Krasikova et al., Nucl Med Biol 2004). Rats bearing Glioma-35-derived rat tumours (homografts) and turpentine-induced inflammatory foci (aseptic abscess) developed in a left hind leg were used. The uptake of radiotracers was measured by direct radiometry of the tissue samples as the percentage of injected dose per gram (% ID/g). Based on these data the tumor-to-muscle or inflammation-to-muscle ratios were calculated using right hind leg as a reference region. The biodistribution of radioactivity was accessed in 40, 60, 120 min after injection (3 rats for each time point for every tracer).

Results and Discussion: Tumor-to-muscle ratios were in range of 0.6-1.8 for 6-FDOPA and in range of 2.2-2.8 for FDG. Accumulation of 6-FDOPA in inflammatory tissue was similar to tumor (inflammation-to-muscle ratio in range of 1.8-2.2) while higher uptake was observed for FDG (inflammation-to-muscle ratio in range of 5.8-9,1).

Conclusion: Preliminary experiments in our animal model shown that 6-FDOPA accumulated less into the inflamed tissue in comparison to FDG. We may assume that the use of this tracer in combination with FDG may allow differentiation of tumour and inflammation.

Acknowledgement: This work was supported by ISTC grant 2780.

Keywords: 6-18F-FDOPA, Inflammation, Tumor, FDG

P392 COMPARISON OF FET, MET UND DEOXYGLUCOSE UPTAKE IN CEREBRAL ABSCESSES USING DUAL-TRACER AUTORADIOGRAPHY IN RATS

D. SALBER, K. HAMACHER[2], G. STOFFELS[3], D. PAULEIT[3], H.H. COENEN[2] and K.J. LANGEN[3]

[1]C. & O. Vogt Institute of Brain Research, Düsseldorf University Hospital, Düsseldorf, Germany; [2]Institute of Neurosciences and Biophysics-Nuclear Chemistry, Forschungszentrum Jülich, GmbH, Jülich, Germany; [3]Institute of Neurosciences and Biophysics-Medicine, Forschungszentrum Jülich, GmbH, Jülich, Germany

Introduction: The PET tracer O-(2-[^{18}F]fluorethyl)-L-tyrosine (FET) is under clinical evaluation for brain tumor imaging. Experimental studies have shown that there is no uptake of FET in inflammatory cells. Recently, however, increased FET uptake was reported in two out of six brain abscesses in humans. In order to further investigate the uptake behaviour of the tracer in inflammatory brain processes we compared the uptake of FET, L-[^{3}H]-methionine (MET) and [^{3}H]-desoxyglucose (DG) in brain abscesses in rats using dual-tracer autoradiography.

Experimental: Cerebral abscesses were induced in 9 CDF-Fischer rats after inoculation of a suspension of staphylococcus aureus into the brain. Five days later FET and MET (n=5) or FET and H-DG (n=4) were injected intravenously. One hour after injection the rats were sacrificed, the brains removed and frozen at -50°C in isopentane. Brains were cut in coronal sections (thickness: 20 μm) and exposed first to ^{3}H-insensitive photoimager plates to measure FET distribution. After decay of ^{18}F, the distribution of MET resp. DG was determined. The autoradiograms were evaluated by regions of interest (ROIs) placed on areas with maximal tracer uptake in the abscess and the contralateral brain. Lesion to brain ratios (L/B) were calculated by dividing the maximal uptake in the lesion and by the mean uptake in the brain. For histological comparison the slices were stained with toluidine blue. Macrophages and reactive astrogliosis were detected using anti-CD68 and anti-GFAP specific antibodies in immunofluorescence.

Results and Discussion: In all animals distinct brain abscesses could be generated. In the area of macrophage infiltration at the rim of the abscesses as demonstrated by anti-CD68 immunofluorescence, high uptake was observed for MET as well as for H-DG (L/B 4.2 $\pm$ 1.2 for MET resp. 3.1 $\pm$ 1,2 for DG). In contrast, FET exhibited only low uptake in CD68-positive cells (L/B 1.4 $\pm$ 0.3). In the penumbra of the abscesses, however, slightly increased uptake was noted for FET (L/B 1.8 $\pm$ 0.3) and MET (L/B 1.8 $\pm$ 0.4) while DG distribution was normal (L/B 1.1 $\pm$ 0.2). Anti-CD68 and anti-GFAP immunofluorescence did not show major abnormalities in those areas.

Conclusion: Our results in experimental brain abscesses confirm that there is no accumulation of FET in macrophages while MET and DG exhibit high uptake in these cells. Slightly increased uptake of both FET and MET may be observed in the penumbra of abscesses. The reason for the latter remains to be elucidated.

Keywords: FET, Abscess

P393 EFFECT OF ANTIDEPRESSANTS ON BINDING OF 5-(^{123}I)A85380 TO NICOTINIC RECEPTORS IN HUMANS

J. CAVANAGH [1], S. PIMLOTT [2], M.F. DEMPSEY [3], J. PATTERSON [3] and D. WYPER [3]

[1]Division of Community Based Sciences, University of Glasgow, Glasgow, United Kingdom; [2]West of Scotland Radionuclide Dispensary, Western Infirmary, Glasgow, United Kingdom; [3]Institute of Neurological Sciences, Southern General Hospital, Glasgow

Introduction: There is growing evidence that nicotinic receptors play a role in depression. As such, imaging nicotinic receptors will become a more useful tool to aid psychiatric diagnosis. Antidepressant drugs have long been known to possess anticholinergic effects, but there is sparse literature as to how antidepressant drugs will affect SPECT ligand binding. Using the radioligand 5-^{123}I-A85380 we investigated in vivo whether selective serotonin reuptake inhibitors (SSRIs) affected binding to $\alpha4\beta2$ nicotinic acetylcholine receptors.

Experimental: The synthesis of 5-^{123}I-A-85380 was achieved via electrophilic iododestannylation of the corresponding tri-n-butyltin precursor, using the oxidant chloramine-T. The 5-^{123}I-A85380 was formulated as 150 MBq in 5 ml in sodium chloride for intravenous injection containing up to 1.5 mg ascorbic acid.

5 patients meeting the criteria for DSM-IV major depression (APA, 1994) were imaged prior to discontinuation of their antidepressant medication then again following the discontinuation and a 6-week washout period. Subjects were imaged at 4 hours post-injection and region of interest analysis was performed using two different regions; occipital cortex and corpus callosum.

Results and Discussion: The 5-^{123}I-A85380 used in this study was produced with an isolated radiochemical yield of 65.8% $\pm$ 5.9 (n = 8), a radiochemical purity of $>$ 98%

The study found that there was no significant difference in the availability of the $\alpha4\beta2$ nicotinic receptor in the presence or absence of SSRIs. This is corroborated by previously reported in vitro binding data. This suggests that 5-^{123}I-A85380 is a suitable ligand for SPECT imaging of $\alpha4\beta2$ nicotinic acetylcholine receptors in patients who are taking an antidepressant.

Additionally, this study carries the implication that antidepressants exert their anticholinergic effects by a mechanism other than competitive inhibition or blockade occurring at receptors other than $\alpha4\beta2$.

Conclusion: SPECT imaging with 5-^{123}I-A-85380 can be used to investigate nicotinic receptors in the brains of depressed patients who are taking SSRIs, without causing a confounding effect.

Acknowledgement: This study was funded by the West of Scotland Research and Development Consortium.

Keywords: 5-I-A-85380, Nicotinic, Depression, Antidepressant, Imaging

P394 ROLE OF ([18]F)FLUORIDE IN PRECLINICAL EVALUATION OF [18]F-LABELLED RADIOTRACERS

N. SAVISTO [1], V. FAGERHOLM [2], J. BERGMAN [1], O. SOLIN [1] and M. HAAPARANTA [2]

[1]Radiopharmaceutical Chemistry Laboratory and Accelerator Laboratory, Turku PET Centre, University of Turku and Åbo Akademi University, Turku, Finland; [2]Preclinical Imaging Turku PET Centre, University of Turku, Turku, Finland

Introduction: Fluorine-18-labelled radiotracers are widely used for PET studies. Many of them will at some point in their metabolism lose their ^{18}F-label. Released [^{18}F]fluoride accumulates in bone, and defluorination of ^{18}F-labelled tracers *in vivo* is therefore monitored by measuring bone uptake as a function of time. In addition, [^{18}F]fluoride is as such used as a bone-scanning agent. However, the kinetics of [^{18}F]fluoride uptake in bone and other organs is not well documented in experimental animals. In this study we determined the biodistribution of [^{18}F]fluoride in healthy rats as a function of time and optimized the chromatographic methods for fluoride analysis.

Experimental: [^{18}F]Fluoride was produced by irradiating ^{18}O-enriched water with protons from an isochronous cyclotron (MGC-20). Radiochemical and radionuclidic purity of the product exceeded 99%. The *ex vivo* biodistribution of ^{18}F-radioactivity in healthy male and female Hsd:SD rats was determined at 15, 30, 60, 120, 240 and 360 min after i.v. injection of [^{18}F]fluoride. At each time point 3 animals were used. The *in vivo* biodistribution was studied by dynamic PET imaging with a HRRT scanner. Chromatographic analysis methods for fluoride were optimised. ^{18}F-distribution in the brain was determined by digital autoradiography.

Results and Discussion: As expected, accumulation of [^{18}F]fluoride in bone was high, ranging from 1.69 ± 0.25%ID/g at 15 min to a maximum of 2.70 ± 0.41%ID/g at 120 min in male rats, and from 1.15 ± 0.03 to 2.46 ± 0.31%ID/g in female rats at the same time points. In plasma, the highest [^{18}F]fluoride levels were measured at 15 min, declining thereafter in both sexes. In most soft tissues [^{18}F]fluoride uptake was higher in females than in males. The highest uptake (%ID/g) up to 30 min was found in kidney > thymus > lung > liver >skin > adrenal gland. At later time points, the uptake (%ID/g) in kidneys, thyroids and eyes exceeded that of the other soft tissues. Low levels of radioactivity were found in all other organs and tissues studied. Interestingly, the [^{18}F]fluoride levels in plasma and brain equilibrated at about 150 min p.i. at a value of approximately 0.5%ID/g. In the brain, [^{18}F]fluoride radioactivity was fairly homogenously distributed.

Conclusion: When assessing the ^{18}F-radioactivity biodistribution of ^{18}F-labelled tracers which release substantial amounts of [^{18}F]fluoride, the heterogeneous biodistribution of [^{18}F]fluoride itself should also be considered.

References: Hein JW, Bonner JF, Brudevold F, Smith FA, Hodge HC (1956) Nature 4545:1295-96.

Keywords: F-18, Fluoride, Biodistribution, Rat

P395 PHARMACOKINETICS OF A FUSION INHIBITOR OF THE HEPATITIS B VIRUS

W. MIER [1], S. URBAN [2], S. KRÄMER [1], M. EISENHUT [3] and U. HABERKORN [1]

[1]Abteilung für Nuklearmedizin, University Clinics of Heidelberg, Heidelberg, Germany; [2]Department of Molecular Virology, University Clinics of Heidelberg, Heidelberg, Germany; [3]Radiopharmaceutical Chemistry, German Cancer Research Centre (DKFZ), Heidelberg, Germany

Introduction: Chronic infection with the human hepatitis B virus (HBV) is still a major health problem to the world's population today. Interference with HBV infection by externally applied fragments of viral surface proteins that interfere with receptor interaction or membrane fusion might allow the development of novel antiviral strategies that interfere with the hepadnaviral entry process, as has been shown for gp-41-derived T 20-peptides in HIV-therapy. Proteins that interfere with the fusion of the virus might be used as diagnostic tracers for viral diseases.

Experimental: We have recently demonstrated that peptides encompassing the 47 terminal amino acids of the N-terminal part of a major envelope protein block HBV infection of primary human hepatocytes with surprising efficacy, at already picomolar concentrations, probably by sustained inactivation of a receptor on hepatocytes (Gripon P, Cannie I, Urban S. Efficient inhibition of hepatitis B virus infection by acylated peptides derived from the large viral surface protein. J Virol. 2005; 79: 1613-22). The biodistribution of the I-125-labelled peptide was determined in RAG-2 mice bearing hepatocytes susceptible to infection with HBV. The stability of the peptide was determined in human serum.

Results and Discussion: A tyrosine bearing derivative of the peptide Myr-GQNLSTSNPLGFFPDHQLDPAFRANT ANPDWDFNPNKDWTPDANKVG-COOH was obtained by Fmoc solid phase synthesis. The peptide was labelled with 125-I using the Chloramine-T method. No significant increase of the I-125-labelled peptide was determined in mice bearing infection susceptible hepatocytes at 1 h post injection. The peptide was cleared by the kidneys that were the major sites of accumulation. However, a high concentration (5.1%ID/g at 1 h post injection) was found in the blood. The biological half live of the peptide was > 60 h in human serum.

Conclusion: Using the labelled lipopeptide we investigated the organ distribution with respect to a specific targeting to the transplanted hepatocytes, as well as the peptide stability in serum. At the levels determined, this preclinical study did not reveal a targeting of the hepatocytes. However, the peptide is circulating in the blood at concentration that is high enough to prevent infections with the virus. It can be speculated that the peptide is protected against degradation due to an association via its lipophilic end to serum proteins. Consequently, the peptide is a promising candidate for future clinical applications, e.g. prevention of HBV reinfection after liver transplantation.

Keywords: Hepatitis, Targeting, Peptides

P396 DOTA CONJUGATION OF A PEPTIDE IDENTIFIED BY PHAGE DISPLAY

W. MIER [1], S. ZITZMANN [2], S. KRAEMER [1], M. EISENHUT [3] and U. HABERKORN [1]

[1]Department of Nuclear Medicine, University of Heidelberg, Heidelberg, Germany; [2]Clinical Cooperation Unit Nuclear Medicine, German Cancer Research Centre (DKFZ), Heidelberg, Germany; [3]Department of Radiopharmaceutical Chemistry, German Cancer Research Centre (DKFZ), Heidelberg, Germany

Introduction: The transfer of peptide sequences identified by screening of phage-displayed libraries to clinical application is often difficult. This study investigated whether coupling of a new peptide FROP-1 to the chelator DOTA resulted in structural restriction and consequently improved binding and stability.

Experimental: The peptide FROP-1 was coupled to the chelator DOTA and labeled with 111In. The structural changes caused by the addition of the chelator were determined by circular dichroism. The properties of this modified peptide were investigated in in vitro binding assays and monitored for kinetics, competition and internalization as well as serum stability. A cell type binding profile was established and the in vivo biodistribution was evaluated in a nude mouse model.

Results and Discussion: When compared to the free peptide without chelator, FROPDOTA revealed different cellular uptake kinetics reaching a maximum at 2 h in vitro. The cells completely accumulated the tracer and competition experiments revealed that 99.4% (FRO82-2 cells), 98.6% (MCF-7 cells) or 99.3% (average for three primary head and neck tumor cell lines) of tracer accumulation could be suppressed, revealing the specificity of this process. The internalization kinetics determined in MCF-7 cells supported this finding: after an incubation time of 180 min the major fraction of FROPDOTA was trapped intracellularly. Serum stability experiments revealed a increase in stability due to the chelator, with a half life of 71 min. Circular dichroism measurements indicated a fixed alpha helix structure of FROPDOTA representing a strong change in secondary structure. In competition binding experiments the binding constant (KD) to FRO82-2 cells was determined to be 494 nM. Despite this avid binding affinity the binding kinetics was found to be too slow to induce an uptake in vivo prior to clearance. Consequently, the biodistribution revealed a rapid renal and hepatobiliary clearance with blood levels dropping from 5.48 $\pm$0.26%ID/g five min p.i. to 0.77 $\pm$ 0.15%ID/g at 135 min p.i.

Conclusion: This study revealed that peptides that are identified by display techniques may be underrated. Careful alteration of their structure will permit going beyond the possibilities that the limited pool of naturally occurring peptides provide for tumor targeting.

Keywords: Peptides, Phare Display, Targeting, Chelators, Oncology

P397 (^{11}C)5-HTP AND (^{18}F)FDOPA: A VIEW ON UPTAKE MECHANISMS AND METABOLISM IN A NEUROENDOCRINE PANCREAS TUMOUR CELL LINE

O.C. NEELS [1], H. TIMMER-BOSSCHA [2], I.P. KEMA [3], K.P. KOOPMANS [1], P.L. JAGER [1], E.G.E. DE VRIES [2], R.A. DIERCKX [1] and P.H. ELSINGA [1]

[1]Nuclear Medicine & Molecular Imaging, UMCG, University of Groningen; [2]Medical Oncology, UMCG, University of Groningen; [3]Pathology & Laboratory Medicine, UMCG, University of Groningen, Groningen, Netherlands

Introduction: Several PET studies on patients with neuroendocrine tumours have been described. In these studies the APUD principle plays a decisive role. The aim of this study is to investigate uptake mechanism of the PET-tracers [^{11}C]5-HTP and [^{18}F]FDOPA in a neuroendocrine cell line by using the AADC inhibitor carbidopa and the LAT1 inhibitor BCH. Metabolism was studied by the use of non-labelled amino acid 5-HTP and several blocking agents and analytical methods.

Experimental: Experiments were performed with cells derived from a human neuroendocrine pancreas tumour (BON). Cells were depleted from internal amino acids by displacing growth medium with PBS-GMC buffer and wash-out for 1 hour. Cells were treated with PBS-GMC buffer containing selective inhibitors as carbidopa, BCH, clorgyline or pargyline. [^{11}C]5-HTP and [^{18}F]FDOPA were added under effect of AADC inhibitor carbidopa (0.08 mM) and intracellular uptake was measured in a time course ranging from 5 to 60 minutes. Intracellular uptake of both PET-tracers was measured for LAT1 inhibitor BCH (0-20 mM) for the time point of 15 minutes. Metabolism was determined by HPLC-analysis by treating cells with MAO inhibitors clorgyline (0.1 mM) and pargyline (0.1 mM) and carbidopa (0.08 mM) and adding non-labelled tracer in equivalent amounts as PET-tracer.

Results and Discussion: [^{11}C]5-HTP and [^{18}F]FDOPA were taken up rapidly. [^{18}F]FDOPA was taken up within 15 minutes (11%) and remained constant up to 60 minutes. [^{11}C]5-HTP uptake was much higher than FDOPA (ratio 5:1) at 60 minutes (60%). For both tracers no significant difference in intracellular uptake was observed in carbidopa-treated and non-treated cells. Nearly depressed intracellular uptake is observed at low concentrations of BCH (1.0 mM) for [^{11}C]5-HTP and [^{18}F]FDOPA. Up to 0.1 mM BCH concentration uptake of [^{11}C]5-HTP is less blocked than for [^{18}F]FDOPA. After 15 and 60 minutes non-labelled 5-HTP (34%/14%) and metabolites 5-HT (6%/3%) and 5-HIAA (60%/83%) can be found in cells while carbidopa inhibited the internal synthesis of 5-HT and 5-HIAA and clorgyline and pargyline blocked selectively 5-HIAA synthesis, however not affecting total cellular uptake.

Conclusion: [^{11}C]5-HTP seems to be superior to [^{18}F]FDOPA in foregut tumours. While the use of carbidopa has a relevant influence in human studies it does not influence *in vitro* tracer uptake. Based on these *in vitro* data, tracer levels seem to reflect LAT1 uptake rather than neurotransmitter synthesis.

Acknowledgement: BON cells were achieved from Sahlgrenska University Hospital, Gothenburg, Sweden.

Keywords: [^{11}C]-5-Hydroxytryptophan, [^{18}F]FDOPA, Neuroendocrine Tumors, APUD, BON Cells

P398 EVALUATION OF (F-18)DFT (5'-DEOXY-5'-(F-18)FLUOROTHYMIDINE) AS A TRACER OF INTRACELLULAR THYMIDINE PHOSPHORYLASE ACTIVITY

J.R. GRIERSON [1], J.S. BROCKENBROUGH [1], J.S. RASEY [2], L.W. WIENS [1], J.L. SCHWARTZ [2], R. JORDAN [2] and H.J. VESSELLE [1]

[1]Radiology, University of Washington, Seattle, WA, USA; [2]Radiation Oncology, University of Washington, Seattle, WA, USA

Introduction: [F-18]DFT was screened as a potential agent for imaging thymidine phosphorylase (TP) activity. This investigation was based on several preliminary observations and predictions, namely: (1) DFT is a TdR (thymidine) analog that should display an initial biodistribution that mirrors thymidine; (2) placement of the label on the sugar ring of DFT eliminates issues with pyrimidine metabolism; (3) inorganic phosphate is the only co-factor needed for DFT to react with TP; (4) DFT is a TP substrate and should not cross react with UPase (uridine phosporylase); (5) TP converts DFT to 2,5-dideoxy-5-fluoro-D-ribose-1-alpha-phosphate (5-FddR-1P), which should be trapped in cells; (6) 5-FddR-1P cannot not be further metabolized according to the normal scheme available to dR-1P (2-deoxyribose-1-alpha-phosphate); (7) DFT cannot be anabolized by nucleoside and nucleotide kinases and; (8) in vivo, DFT metabolism in blood would form 5-FddR-1P, but this metabolite should remain there or be excreted.

Experimental: Two human cell lines, A549 (human lung carcinoma) and U937 (human lymphoma cell line with monocytic characteristics), with cytosolic thymidine phosphorylase (TP) activity were used to evaluate [F-18]DFT. Tracer uptake and washout experiments were conducted.

Results and Discussion: Intracellular metabolism of DFT led to the exclusive production of 5-FddR-1P, in analogy to the metabolism of thymidine to dR-1P. A549 cells showed the highest production rate of 5-FddR-1P. After 40 minutes of DFT exposure, the relative intracellular concentration of this metabolite was more than 7-fold higher than of its precursor in the incubating media. A much smaller, 2-fold, concentration was seen with U937 cells. Despite the specific accumulation of intracellular radioactivity, it subsequently effluxed from cells into tracer-free media within 1h. Radioactivity lost from cells was predominantly in the form of a neutral lipophilic species, presumed to be a deoxynucleoside, and was not the dephosphorylated fluoro-sugar.

Conclusion: Overall, the results suggest that [F 18]DFT would not be an effective agent for imaging TP expression in vivo because its initial metabolite undergoes further conversion to a diffusible product.

Acknowledgement: This work was supported by NIH grant RO1 CA 115559.

Keywords: 5'-Deoxy-5'-[F-18]Fluorothymidine, [F-18]DFT, Thymidine Phosphorylase, Fluorine-18, PET

P399 SPECIES DEPENDENCE OF (^{64}Cu)Cu-BIS(THIOSEMICARBAZONE) COPPER(II) RADIOPHARMACEUTICAL BINDING TO SERUM ALBUMIN

N.E. BASKEN, C.J. MATHIAS and M.A. GREEN

Industrial and Physical Pharmacy, Purdue University, West Lafayette, IN, USA

Introduction: Protein binding is a critical factor that influences the pharmacokinetics of radiotracers and, in part, impacts their distribution between blood and other tissues. The clinical utility of agents requiring high first-pass extraction may be compromised if extensive protein binding impedes distribution of the tracer out of the plasma compartment. Further, the affinity of radiopharmaceuticals for serum albumin can vary considerably between species. This is an important consideration when evaluating studies using animal models to predict product performance in humans. We present here additional results characterizing the species and compound dependence of albumin binding with small, neutral, lipophilic copper(II) bis(thiosemicarbazone) radiopharmaceuticals.

Experimental: ^{64}Cu-labeled pyruvaldehyde bis(N^4-methylthiosemicarbazonato)copper(II) (Cu-PTSM), ethylglyoxal bis(thiosemicarbazonato)copper(II) (Cu-ETS), and diacetyl bis(N^4-methylthiosemicarbazonato)copper(II) (Cu-ATSM) were synthesized, and their affinites for the serum albumins of several species quantified by ultrafiltration binding assays. The albumin solutions were prepared and analyzed at a concentration of 40 mg/mL.

Results and Discussion: The figure shows a subset of our data for five of the species studied (human, dog, rat, baboon, and pig). Cu-PTSM and Cu-ATSM show pronounced species-dependent variations in the level of their binding to serum albumin. Additionally, for each species, Cu-PTSM and Cu-ATSM exhibit higher binding (lower % free) than Cu-ETS. Human serum albumin (HSA) provides a dramatic example of protein binding differences between these three structurally similar copper(II) chelates. Approximately 95% of available Cu-PTSM or Cu-ATSM is bound to HSA, compared to only 60% binding in the case of Cu-ETS. By contrast, these three tracers are very similar in their affinity for canine serum albumin.

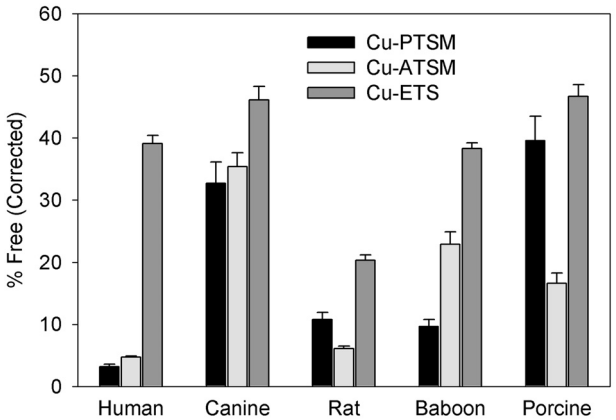

Fig. 1. Interspecies variation of Cu-chelate binding to serum albumin (40 mg/ml).

Conclusion: Quantifying the extent of radiopharmaceutical binding to serum proteins is an important factor to consider when evaluating the performance of a radiotracer. This data may further be used to improve the predictive power of pre-clinical studies performed in animal models.

Acknowledgement: This work was supported by National Institutes of Health (R01-CA0924403) and a fellowship from the Purdue Research Foundation. The production of Cu-64 at Washington University School of Medicine was supported by NIH grant R24 CA86307.

Keywords: Copper-64, Cu-PTSM, Cu-ETS, Cu-ATSM, Albumin Binding

P400 (^{11}C)(*R*)-(-)-RWAY – TEST FOR POTENTIAL RACEMIZATION *IN VIVO* WITH CHIRAL HPLC

S.S. ZOGHBI, J.A. MCCARRON, H.U. SHETTY, J.S. LIOW, J.S. HONG, E. TUAN, R.B. INNIS and V.W. PIKE

MIB, NIMH, Bethesda, MD, USA

Introduction: [^{11}C](*R*)-(-)-RWAY (**1**) is used to image serotonin subtype-1 (5-HT_{1A}) brain receptors. Conceivably, this radioligand, which has a potentially labile benzylic hydrogen at its chiral center, inverts to [^{11}C](*S*)-(+)-RWAY *in vivo*, which may then become a brain impurity. Curiously, there appears to be no previous report testing for racemization *in vivo* following administration of any homochiral PET radioligand. Such racemization, if it were to occur, might in certain cases cause biomathematical modeling difficulties in the acquired PET data. Here we aimed to develop a chiral radio-HPLC method for [^{11}C](*R*)-(-)-RWAY to test for its racemization *in vivo*.

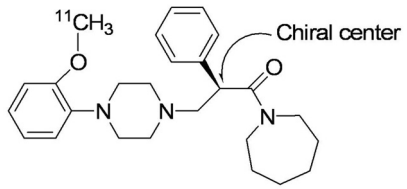

(1)

Experimental: [^{11}C]RWAY enantiomers were synthesized as previous [1]. Enantio-purities monitored by HPLC on Chiralpak AD column (250 × 4.6 mm) eluted with *n*-hexane-isopropanol- Et_3N (95: 5: 0.1, by vol.). Effects of liquid-liquid extraction methods on racemization of (*R*)-(-)- and (*S*)-(+)-RWAY were studied in: water; 0.9% NaCl, (with and without basifying HCO_3^-); 0.15 M phosphate buffer (pH, 7.4); rodent plasma and whole blood; and, brain, kidney and liver homogenates at 37°C. Ethyl acetate, *n*-hexane or HPLC mobile phase were extraction solvents. Each no-carrier-added enantiomer (~680 μCi, $n = 3$) was injected into P-gp knockout mice. Tissue extracts, 30 min post ID, were analyzed by chiral radio-HPLC. Carrier-added enantiomers (5 mg/kg) were injected into rats. Brain, blood and urine were analyzed at 60 min post ID by chiral HPLC and separated peaks examined by LC-MS-MS. Blood and urine were also collected up to 90 min after [^{11}C](*R*)-(-)- or [^{11}C](*S*)-(+)-RWAY (~7 mCi) injection into rhesus monkey and analyzed by chiral radio-HPLC.

Results and Discussion: (*R*)-(-)- (t_R 17 mL) and (*S*)-(+)-RWAY (t_R 11 mL) were completely resolved by chiral HPLC. Mobile phase was most efficient (up to 92%) to extract RWAY from biological samples. No racemization of radioligand was found in electrolytic solutions or the biological samples *in vitro*. *Ex vivo* rodent brain, blood and urine samples demonstrated low conversion (0.2–0.4% ID) of the (*R*)-(-)- to the *S*-(+)-RWAY (identity confirmed with LC-MS-MS) over a period of 60 min. No racemization occurred in monkey.

Conclusion: Quantification of [^{11}C]-RWAY enantiomers in biological samples was feasible by chiral radio-HPLC. (*R*)-(-)-RWAY underwent racemization *in vivo* to a very low but detectable extent in rodents, but not in a monkey.

Acknowledgement: Supported by the Intramural Research Program of the NIH/NIMH.

Keywords: Racimization, [^{11}C](R)-(-)-RWAY, Enatioselective Radio-HPLC, Chiral Radio-HPLC

P401 EFFECT OF MULTIDRUG RESISTANCE-ASSOCIATED PROTEIN 4 AND 5 ON THE EFFLUX OF (^{18}F)FLT

D. NIEDZIELSKA [1], P. MIKECZ [1,3], O. SCHULZE [1], R. BUCHERT [1], U. SCHUMACHER [2] and W. BRENNER [1]

[1]Department of Nuclear Medicine, University Medical Center Hamburg-Eppendorf, Hamburg, Germany; [2]Department of Anatomy II. Experimental Morphology, University Medical Center Hamburg-Eppendorf, Hamburg, Germany; [3]Institute for Nuclear Medicine, University of Debrecen, Debrecen, Hungary

Introduction: 3'-Deoxy-3'-[F-18]fluorothymidine (FLT) is a promissing tracer for imaging cell proliferation in vivo using positron emission tomography (PET). A currently published in vitro study showed, that up to 50% of FLT could be effluxed into media. These extrude mechanisms could be caused by a family of ATP-dependent efflux pumps, the Multidrug Resistance associated-Protein (MRP) transporters. The prospective candidates of that family are MRP4- and MRP5-transporters, which extrude purines or pyrimidines as well as their anologues. The aim of our in vitro study was to investigate the role of MRP4/5-transporters in the efflux of FLT and its metabolites.

Experimental: For the in vitro experiments we used both wildtype (wt) and MRP4/MRP5-transfected human embryonal kidney cells (HEK293). After 1h of incubation with FLT (100 kBq/well) and thorough washing, cell pellets were counted. For determination of the efflux a set of identically treated cells was incubated for another 1 hour in FLT-free medium in the presence or absence of a specific MRP4-inhibitor (prostaglandine E1, PGE1) or inhibitor of nucleosid transport (nitrobenzylmercaptopurine riboside, NBMPR). The intra- and extracellular metabolites were analysed with HPLC.

Results and Discussion: The efflux of FLT (% of total uptake, n = 15 each, mean ± SD) in wtHEK was 53 ± 5,% and in MRP5-transfected cells 64 ± 6% ($p < 0.05$). MRP5-transfected cells showed independently of specific inhibitor treatment a relatively high efflux of FLT-monophosphate (FLTMP) up to 44 ± 2% compared to 12 ± 2% in wtHEK. On the contrary, there was no significant difference in total efflux between MRP4-transfectants and wt-cells, although the distribution of metabolites of FLT showed similar patterns as observed in MRP5 (Table 1).

Cell line	Without Inhibitor			With Inhibitor		
	FLT%	FLTMP %	FLTDP/TP %	FLT %	FLTMP %	FLTDP/TP %
HEK	84±2	12±2	4±1	82±3	13±1	5±2
MRP5-HEK	50±2	44±2	6±1	53±11	41±8	7±3
MRP4-HEK	52±2	44±1	5±2	58±1	40±3	6±1

Conclusion: The MRP5-transfected cells showed a significantly higher total efflux than wt-cells with a relative increase in effluxed FLTMP compared to FLT. This shift in metabolite efflux is expected due to the fact that MRP5 acts as nucleotide pump. MRP4 on the contrary did not increase the total efflux of metabolites although a shift towards FLTMP was observed, too. These results implicate a significant involvement of MRP5-transporters in FLT efflux while MRP4, although acting as FLTMP transporter, does not seem to have major impact on total FLT efflux.

Keywords: [F-18]FLT, Multidrug Resistance-Associated Proteins

P402 MOLECULAR IMAGING AND CONTRAST AGENT DATABASE (MICAD): A COMPONENT OF THE NIH ROADMAP

B. BECK [1], S. BRYANT [1], K.T. CHENG [1], W.C. ECKELMAN [1], K.H. LEUNG [1], E. LUTANIE [1], J. MCENTYRE [1], A. MENKENS [2] and D. SULLIVAN [2]

[1]National Center for Biotechnology Information, National Institutes of Health, Bethesda, MD, USA; [2]National Cancer Institute, National Institutes of Health, Bethesda, MD, USA

Introduction: MICAD (http://micad.nih.gov) is a freely accessible online source of scientific information on *in vivo* molecular imaging agents. It has been developed as a key component of the Molecular Libraries and Imaging (MLI) program of the National Institutes of Health (NIH) Roadmap for Medical Research in the 21st century. The MLI program is a component of the NIH Roadmap that addresses the critical issue of finding new pathways to discovery by supporting the emerging field of molecular imaging.

Experimental: As a part of the MLI program, MICAD focuses on providing critical and timely scientific information to promote the research of molecular imaging agents. The MICAD team is composed of NIH staff who have been working with the guidance of a trans-NIH panel of experts in the field of molecular imaging. MICAD is designed to provide concise, up-to-date, and the most relevant information of molecular imaging agents to the basic and clinical research community. The database includes, but is not limited to, agents developed for positron emission tomography, single photon emission computed tomography, magnetic resonance imaging, ultrasound, computed tomography, optical imaging, planar radiography, and planar gamma imaging.

Results and Discussion: The information is summarized in 5 major sections: background, synthesis, *in vitro* studies, animal studies (rodents, other non-primate mammals, non-human primates), and human studies. MICAD catalogs information describing the chemical/radiochemical synthesis, specificities, biological activities, and medical applications of imaging probes for a wide range of diseases and biological functions. The database also features literature references with links to MEDLINE/PubMed, chemical structures with links to PubChem, and additional related resources at NCBI.

Conclusion: The MICAD website was officially launched in September 2005. It currently contains more than 222 agents and is fully searchable. All molecular imaging agents that are published in peer-reviewed literature will eventually be included.

Acknowledgement: This project is supported by the Intramural Research Program of the NIH.

Keywords: MICAD, Molecular Imaging, Online Database, Radiopharmacology

P403 (^{18}F)FE@CIT: METABOLIC CONSIDERATIONS

D.E. ETTLINGER [1], W. WADSAK [1], L.K. MIEN [1,2,3], D. HAEUSLER [1,2], R.R. LANZENBERGER [3], R. DUDCZAK [1], K. KLETTER [1] and M. MITTERHAUSER [1,2]

[1]Department of Nuclear Medicine, Medical University of Vienna, Vienna, Austria; [2]Department of Pharmaceutical Technology and Biopharmaceutics, University of Vienna, Vienna, Austria; [3]Department of Psychiatry, Medical University of Vienna, Vienna, Austria

Introduction: In the last decade radiolabeled tropane analogs based on β-CIT have proven indispensable for the imaging of the dopamine transporter (DAT). However, further improvements in their pharmacodynamic and pharmacokinetic features are desirable. Aim of this study was to (1) evaluate and compare the metabolic stability of β-CIT (2β-carbomethoxy-3β-(4-iodophenyl)tropane), FP-CIT (N-(3-fluoropropyl)-3β-(4-iodophenyl)nortropane-2β-carboxyacid-methylester) and FE@CIT (2β-carbo-2'-fluoroethyloxy-3β-(4-iodophenyl)tropane) against esterases and to (2) evaluate specificity and selectivity of FE@CIT compared to β-CIT and FP-CIT using autoradiographic methods.

Experimental: In-vitro assays were performed using different concentrations of β-CIT, FP-CIT and FE@CIT (60, 120, 180, 240 and 360 μmol) with a constant concentration of esterase (80 I.U., 37°C in 1000μl PBS). Samples were taken after 0, 60, 120, 180, 240, 300 and 360 min, precipitated with ice-cold methanol (1+2) and centrifuged for 4 min at 10000 rpm to separate proteins. The obtained supernatant was analysed by qualified HPLC methods. In-vitro autoradiography was performed on coronal 20μm brain sections obtained from 75 days old male Wistar rats. Brain slices were preincubated to block the serotonin (SERT) and norepinephrine transporter (NET) and with different concentrations of β-CIT, FP-CIT and FE@CIT to test specificity. After incubation with [^{123}I]β-CIT, [^{123}I]FP-CIT or [^{18}F]FE@CIT brain slices were analysed using a Packard InstantImager.

Results and Discussion: The in-vitro assays showed Michaelis-Menten constants of 175.2 μmol for β-CIT, 182.6 μmol for FE@CIT and 521.4 μmol for FP-CIT, respectively. The limiting velocities (v_{max}) were similar: 0.1005 μmol/min (β-CIT), 0.1418 μmol/min (FE@CIT) and 0.1308 μmol/min (FP-CIT), respectively. This implies a significant increased esterase stability of FP-CIT compared to β-CIT and FE@CIT ($p < 0.01$ compared to β-CIT and $p < 0.03$ compared to FE@CIT, respectively). Differences between β-CIT and FE@CIT showed no significance. Autoradiographic analyses revealed a good correlation between DAT-rich regions and the uptake pattern of FE@CIT.

Conclusion: (1) In vitro experiments evinced, that FE@CIT has a stability against esterases comparable to that of β-CIT. (2) The data obtained from in-vitro autoradiography proved, that FE@CIT shows uptake in DAT-rich regions.

Stability experiments together with in-vitro autoradiographic findings support the further evaluation of [^{18}F]FE@CIT for positron emission tomography.

Acknowledgement: The project was supported by the Austrian ONB-fund number 11439.

Keywords: β-CIT, [^{18}F]FE@CIT, Dopamine Transporter, Autoradiography, Michaelis-Menten Kinetics

P404 IN VITRO BINDING CHARACTERISTICS OF DIFFERENT A_{2A} ADENOSINE RECEPTOR LIGANDS IN RAT, MOUSE AND PIG BRAIN AUTORADIOGRAPHY

W. SIHVER and A. SCHULZE

Institute of Nuclear Chemistry, Research Center Juelich, Juelich, Germany

Introduction: The neuronal A_{2A} adenosine receptor (A_{2A}AR) binds the neuromodulator adenosine with high affinity. Since A_{2A}ARs are involved in central movement control, the aim is to develop applicable A_{2A}AR ligands to investigate patients with movement disorders like Parkinson using imaging methods like PET. Based on preclinical data of tritiated ligands their suitability for *in vivo* application can be pre-estimated.

Due to promising *in vitro* results of the A_{2A}AR antagonist [^{3}H]MSX-2 with rat brain membranes (Müller et al., 2000) we aimed to confirm the A_{2A}AR binding distribution of [^{3}H]MSX-2 by autoradiography and compared its binding parameters with those of known ligands such as [^{3}H]ZM241385 (A_{2A}AR antagonist), [^{3}H]CGS21680 (A_{2A}AR agonist) and [^{3}H]NECA (nonselective A_1,A_{2A}AR agonist).

Experimental: For autoradiography, frozen rat and pig brain sections were incubated with different concentrations of tritiated ligand and thereafter washed in buffer. Dried sections were exposed to tritium sensitive phosphor image plates and scanned with a laser phosphor imager. Data from regions of interest were obtained by an image analyzer program, transferred to Excel and further analyzed with a non-linear curve-fitting analysis program.

Results and Discussion: The distribution of [^{3}H]MSX-2 binding showed a distinct accumulation in the striatum of mouse, rat and pig brain. The binding in other brain regions (cortex and cerebellum) was nonspecific. The nonspecific binding was highest for [^{3}H]MSX-2 ($\geq$ 50%) followed by [^{3}H]CGS21680, [^{3}H]NECA and [^{3}H]ZM241385. [^{3}H]CGS21680 and [^{3}H]ZM241385 showed also typical binding distribution for the A_{2A}AR in striatum. However, low specific [^{3}H]CGS21680 binding was measured as well in cortex and cerebellum. [^{3}H]NECA labeled both A_1 and A_{2A}ARs.

Saturation data reveal the highest affinity for [^{3}H]ZM241385 followed by [^{3}H]MSX-2, [^{3}H]NECA and [^{3}H]CGS21680. [^{3}H]NECA + 1 μM DPCPX displaced the A_1 binding and decreased the binding in cortex and cerebellum. The highest amount of A_{2A}AR binding sites was measured in mouse striatum followed by rat and pig striatum. The amount of binding sites measured with [^{3}H]MSX-2 was about 10 fold lower compared with the other tritiated ligands which is attributed to a fast racemization of the substance and the generation of metabolites during incubation.

Conclusion: [^{3}H]MSX-2 bound with high affinity specific in the A_{2A}AR containing striatum, but the nonspecific binding was high and the amount of binding sites unexpected low. Thus, the lipophilic, fast racemizing radioligand MSX-2 appears to be less suitable for *in vitro* binding assays compared with the A_{2A}AR ligands [^{3}H]ZM241385 and [^{3}H]CGS21680. Hence, an *in vivo* application of this ligand is likely to be unsuitable.

References: Müller CE, Maurinsh J, Sauer R. Eur J Pharm Sci 2000, 10:259-65